



**Fermi National Accelerator Laboratory**

**FERMILAB-Conf-96/090-A**

## **New Guises for Old Dark-Matter Suspects**

**Edward W. Kolb**

*Fermi National Accelerator Laboratory  
P.O. Box 500, Batavia, Illinois 60510*

**April 1996**

*Proceedings of the Relativistic Astrophysics: A Conference in Honour of  
Igor Novikov's 60th Birthday,*  
**To be Published by Cambridge University Press**

## **Disclaimer**

*This report was prepared as an account of work sponsored by an agency of the United States Government. Neither the United States Government nor any agency thereof, nor any of their employees, makes any warranty, expressed or implied, or assumes any legal liability or responsibility for the accuracy, completeness, or usefulness of any information, apparatus, product, or process disclosed, or represents that its use would not infringe privately owned rights. Reference herein to any specific commercial product, process, or service by trade name, trademark, manufacturer, or otherwise, does not necessarily constitute or imply its endorsement, recommendation, or favoring by the United States Government or any agency thereof. The views and opinions of authors expressed herein do not necessarily state or reflect those of the United States Government or any agency thereof.*

# New Guises for Old Dark-Matter Suspects

By EDWARD W. KOLB

NASA/Fermilab Theoretical Astrophysics Group  
Fermi National Accelerator Laboratory, Box 500, Batavia, Illinois, 60510, USA

The three most popular suspects for particle dark matter are massive neutrinos, axions, and supersymmetric relics. There are now well developed early-universe plots capable of placing each of the suspects at the scene today to be the dark matter of the universe. Because Igor Novikov has contributed in a fundamental way to the idea of a neutrino-dominated universe and knows that story well, I thought he would like to hear something about the other two suspects. But rather than retelling the standard story, I will point out that there may be new twists to the dark matter story, and that old, familiar suspects may hide in unfamiliar guises.

---

## 1. Introduction

One of the simplest questions one might ask about the universe is, “What is it made of?” It is somewhat of an embarrassment for modern cosmologists to be forced to answer the question with the shrug of the shoulders. Although today we see more of the universe than ever before, everything we do see reinforces the fact that there is more to the universe than meets the eye. On scales as small as our galaxy to scales as large as the Hubble radius, most of the mass of the universe seems to be invisible to us. The nature of the ubiquitous dark matter is perhaps the most fundamental question in cosmology today.

Of particular interest to cosmologists interested in the early universe is the possibility that some fraction of the dark matter is non-baryonic, in the form of some species of elementary particle. In most talks on particle dark matter, the first step in the investigation is to round up the usual suspects for identification. At the top of the most-wanted list is the neutrino. Of all the suspects for dark matter, the neutrino is the only one *known* to exist. A mass for the neutrino even as small as a few eV would mean that the neutrino is dynamically important in understanding the formation and evolution of structure in the present universe. Furthermore, without a known principle to require the neutrino to be massless, the neutrino cannot use the alibi that it is naturally massless.†

There is still reasonable doubt about neutrinos as dark matter because it is very hard to construct a scenario where light neutrinos, by themselves, are responsible for structure formation. The problem is that by the time neutrinos would come to dominate the mass of the universe and structure would begin to form, they would have travelled a rather large distance since they first decoupled in the early universe. Because of collisionless phase mixing (or Landau damping), initial perturbations on scales smaller than the free-streaming length,  $20 \text{ Mpc} \times (30 \text{ eV}/m_\nu)$  for neutrinos of mass  $m_\nu$ , would be suppressed. Such a dark matter species with a relatively large velocity just before matter domination, like a light neutrino species, is known as hot-dark matter, or HDM for short.

In order to develop large-scale structure from small initial seeds, most cosmologists favor a type of dark matter known as cold dark matter, or CDM. The matter is called cold, because at the time when the universe first became matter dominated the dark matter was extremely nonrelativistic, and the collisionless damping length was smaller than any scale of astrophysical interest. The list of dark-matter suspects is very long, exceeding in number even the number of characters in a classic Russian novel. But two

† There is no symmetry principle that demands the neutrino must be massless in the way that gauge invariance implies that the photon must be massless.

on the CDM list might be characterized as “prime” suspects: axions and supersymmetric relics. These are the two I will discuss in this talk.

Before starting, it is useful to dispense with the preliminary definitions. It is convenient to express the present mass density of a particle species in terms of its contribution to something known as the critical density. If the density of a matter-dominated universe is greater than the critical density, the universe will eventually recollapse, while if the density is less than the critical density the universe will expand forever. In terms of Hubble’s constant  $H_0$  and Newton’s constant  $G$ , the critical density is  $\rho_C \equiv 3H_0^2/8\pi G = 1.88h^2 \times 10^{-29} \text{ g cm}^{-3}$ . The annoying factor of  $h$  accounts for the imprecision in our knowledge of Hubble’s constant:  $H_0 = 100h \text{ km s}^{-1} \text{ Mpc}^{-1}$ . The energy density in some species “ $i$ ” is given as a ratio to the critical density, and denoted as  $\Omega_i \equiv \rho_i/\rho_C$ .

## 2. Supersymmetric relics

### 2.1. *Supersymmetry and Supersymmetry breaking*

There are two fundamental reasons for believing that nature is supersymmetric. The first reason is that supersymmetry can rescue the standard electroweak model from the embarrassment of finely tuned coupling constants. The standard electroweak model employs fundamental scalars, usually referred to as “Higgs” scalars, to break the gauge symmetry spontaneously. But scalar particles have very bad ultraviolet behavior, which has the effect of dragging the electroweak Higgs mass up to the mass scale of any encompassing theory, such as a grand-unified theory. Thus, unless coupling constants are very finely tuned or some other dynamics enters the picture, light scalar masses (of order the electroweak scale) would not be possible. Supersymmetry (SUSY) is an example of “some other dynamics.” Because of the relative factor of  $-1$  between fermionic and bosonic loops, the addition of fermionic loops can mitigate the bad ultraviolet behavior of scalar loops. The way to realize this possibility is if for every boson there is a corresponding fermion appearing in the calculation of the quantum corrections to the Higgs mass.

This correspondence between fermions and bosons implies that both fermions and bosons appear in multiplets, and they are transformed into each other by supersymmetry transformations. Thus, SUSY is intimately related to Poincaré symmetry. In fact, the commutator of SUSY transformations generates the momentum operator. SUSY is the only known way to unify spacetime and the internal symmetries of the  $S$ -matrix. Thus, SUSY seems to be a fundamental part of any attempt to unify gravity with the fundamental forces. This aesthetic reason is the second motivation for SUSY.

The particular realization of SUSY I will consider is the supersymmetric extension of the standard model. Although this model, the minimal supersymmetric standard model (MSSM), has many parameters in addition to the plethora of parameters of the non-symmetric version of the standard model, it is sufficiently restrictive to have some predictive power.

Of course in nature SUSY is broken—there is no massless fermionic photon for instance. I will return to the question of SUSY breaking in a moment. But the first relevant issue for SUSY dark matter is the existence of something known as  $R$ -parity, a discrete multiplicative symmetry. The  $R$ -parity of a particle is given in terms of its spin  $S$ , baryon number  $B$  and lepton number  $L$ , by  $R = (-1)^{3(B-L)+2S}$ . Known particles all have even  $R$ -parity, while their SUSY partners are all  $R$ -odd particles. If  $R$ -parity is conserved, then the lightest  $R$ -odd color singlet (LROCS) must be stable—and hence a candidate for dark matter. There are inconveniences with any theory if  $R$ -parity is broken. Rapid proton decay, for instance. If one works hard enough these difficulties can be overcome, but

the assumption of exact  $R$ -parity is very attractive and naturally leads to dark matter candidates. So I will assume exact  $R$  parity.

Now let's return to the issue of SUSY breaking. The details of SUSY breaking will determine the identity of the LSP, as well as its mass and interaction strength. Unfortunately, essentially nothing is known about SUSY breaking. The only reasonable constraint one might imagine is that any SUSY-breaking Lagrangian terms must have mass dimension less than four.† Since we have no other choice, let's consider all possible dimension-two and dimension-three SUSY-breaking terms consistent with gauge and Lorentz symmetry:

$$\begin{aligned} \Delta\mathcal{L}(\text{SUSY BREAKING}) = & -m_1^2|H_1|^2 - m_2^2|H_2|^2 - m_{12}^2(H_1H_2 + H_1^*H_2^*) \\ & -\tilde{Q}_{Li}^\dagger(M_Q^2)_{ij}\tilde{Q}_{Lj} - \tilde{u}_{Ri}^\dagger(M_u^2)_{ij}\tilde{u}_{Rj} - \tilde{d}_{Ri}^\dagger(M_d^2)_{ij}\tilde{d}_{Rj} - \tilde{L}_{Li}^\dagger(M_L^2)_{ij}\tilde{L}_{Lj} - \tilde{e}_{Ri}^\dagger(M_e^2)_{ij}\tilde{e}_{Rj} \\ & -H_2\tilde{Q}_{Li}(h_uA_u)_{ij}\tilde{u}_{Rj} - H_1\tilde{Q}_{Li}(h_dA_d)_{ij}\tilde{d}_{Rj} - H_1\tilde{L}_{Li}(h_eA_e)_{ij}\tilde{e}_{Rj} \\ & -\frac{1}{2}M_1\widetilde{B}\widetilde{B} - \frac{1}{2}M_2\widetilde{W}^a\widetilde{W}^a - \frac{1}{2}M_3\widetilde{G}^a\widetilde{G}^a. \end{aligned} \quad (2.1)$$

The tilde superscript denotes the SUSY partner of familiar particles:  $\tilde{e}$  is the selectron,  $\tilde{d}$  is the down squark,  $\widetilde{G}^a$  are the gluino fields,  $\widetilde{W}^a$  and  $\widetilde{B}$  are the supersymmetric partners of the familiar  $SU(2)$  and  $U(1)$  gauge fields, and  $\tilde{Q}$  and  $\tilde{L}$  are  $SU(2)$  doublets containing the SUSY partners of left-handed quarks and leptons. The fields  $H_1$  and  $H_2$  are the two Higgs necessary in SUSY. The parameters  $M_{..}^2$  and  $A_{..}$  are  $3 \times 3$  symmetric matrices. The matrix  $A_{..}$  has mass dimension one. Note that the operators appearing in the first two lines of (2.1) are operators of mass dimension two, while the last two lines contain operators of mass dimension three.

The usual procedure is to choose a set of parameters including the constants appearing in (2.1), requiring that the resulting low-energy theory leads to the usual standard model. The choice of these mass parameters, along with the Higgsino mass parameter  $\mu$ , results in a mass matrix for the neutralinos: the bino  $\widetilde{B}$ , the zino  $\widetilde{W}^3$ , and the Higgsinos  $\widetilde{H}_1^0$  and  $\widetilde{H}_2^0$ . In terms of the mass of the  $Z$ , the weak mixing angle  $\theta_W$ , and  $\tan\beta$  (the ratio of the vacuum expectation values of the two Higgs fields responsible for electroweak symmetry breaking), the neutralino mass matrix in the basis  $(\widetilde{B}, \widetilde{W}^3, \widetilde{H}_1^0, \widetilde{H}_2^0)$  is given as

$$\begin{pmatrix} M_1 & 0 & -m_Z \cos\beta \sin\theta_W & m_Z \sin\beta \sin\theta_W \\ 0 & M_2 & m_Z \cos\beta \cos\theta_W & -m_Z \sin\beta \cos\theta_W \\ -m_Z \cos\beta \sin\theta_W & m_Z \cos\beta \cos\theta_W & 0 & -\mu \\ m_Z \sin\beta \sin\theta_W & -m_Z \sin\beta \cos\theta_W & -\mu & 0 \end{pmatrix}. \quad (2.2)$$

The SUSY-breaking masses  $M_1$  and  $M_2$  are commonly assumed to be of order  $m_Z$  or larger, and if the SUSY model is embedded in a grand unified theory, then  $3M_1/M_2 = 5\alpha_1/\alpha_2$ . If we assume the relation between  $M_1$  and  $M_2$ , then there are three parameters in the neutralino mass matrix:  $\mu$ ,  $\tan\beta$ , and  $M_{1/2}$  (the zino-bino mass parameter).

Now the game is set: for a given set of parameters, diagonalize the mass matrix, find the mass of the lightest supersymmetric particle and its field content (of course in general it is a linear combination of the four neutralino fields), determine its annihilation cross section, and put the above information into the freeze-out machinery to determine the relic abundance.

Different groups who study the problem come up with slightly different composite

† Dimension-four SUSY-breaking terms suffer from the bad ultraviolet behavior we are trying to fix.

sketches for the dark matter suspect. Some believe the particle content is mostly Higgsino, while some find mostly bino. However just about all groups find a relatively large mass for the suspect, between 30 and several hundred GeV.

In this part of the talk† I would like to propose a different picture for the wanted poster: a particle of low mass (500 MeV to 1.6 GeV) and “photino-like,” with an  $SU(2) \times U(1)$  content almost identical to the photon.

The motivation for this light photino comes from our lack of knowledge about SUSY-breaking. Referring to the SUSY-breaking terms in (2.1) we see that there are dimension-two and dimension-three terms. There are theoretical reasons to believe that dimension-three terms might be much smaller than the dimension-two terms. It appears difficult to break SUSY dynamically in a way that produces dimension-three terms while avoiding problems associated with the addition of gauge-singlet superfields. In models where SUSY is broken dynamically or spontaneously in the hidden sector and there are no gauge singlets, all dimension-three SUSY-breaking operators in the effective low-energy theory are suppressed compared to SUSY-breaking scalar masses by a factor of  $\langle \Phi \rangle / m_{Pl}$ , where  $\langle \Phi \rangle$  is the vacuum expectation value of some hidden-sector field and  $m_{Pl}$  is the Planck mass. Thus, dimension-three terms may not contribute to the low energy effective Lagrangian. This would imply that at the tree level the gluino is massless, and the neutralino mass matrix is given by (2.1) with vanishing (00) and (11) entries. However, non-zero contributions to the gluino mass and the neutralino mass matrix come from two sources: radiative corrections such as the top-stop loops for the gluino and neutralinos, and “electroweak” loops involving higgsinos and/or winos and binos for the neutralinos (but not for the gluino).

The generation of radiative gaugino masses in the absence of dimension-three SUSY breaking was studied by Farrar and Masiero. They found (taking  $\mu \gtrsim 40$  GeV) that as the typical SUSY-breaking scalar mass,  $M_0$ , varies between 100 and 400 GeV, the gluino mass ranges from about 700 to about 100 MeV, while the photino mass ranges from around 400 to 900 MeV. This estimate for the photino mass should be considered as merely indicative of its possible value, since an approximation for the electroweak loop is strictly valid only when  $\mu$  and  $M_0$  are much larger than  $m_W$ . The other neutralinos are much heavier, and the production rates of the photino and the next-lightest neutralino in  $Z^0$  decay are consistent with all known bounds.

The conclusion is that light gluinos and photinos are quite consistent with present experiments, and result in a number of striking predictions. One prediction is that the photino  $\tilde{\gamma}$  should be the relic  $R$ -odd particle, even though it may be more massive than the gluino. This is because below the confinement transition the gluino is bound with a gluon into a color-singlet hadron, the  $R^0$ , whose mass (which is in the 1 to 2 GeV range when the gluino is very light) is greater than that of the photino. In this scenario, LSP is an ambiguous term: the gluino is lighter than the photino, although the photino is lighter than the  $R^0$ . As discussed above, a more relevant term would be LROCS—*lightest R-odd color singlet*.

However, models with light gauginos were widely thought to be disallowed because it had been believed that in such models the relic density of the lightest neutralino would exceed cosmological bounds unless  $R$ -parity would be violated allowing the relic to decay. In the next subsection I will rehash that argument, and then point out how the restriction can be evaded if the  $R^0$  mass is close to the  $\tilde{\gamma}$  mass (here “close” means within a factor of two).

† Reference to all the material presented here can be found in Farrar and Kolb (1996) and Chung, Farrar, and Kolb (1996)

2.2. *Self-annihilation and freeze out*

The reaction rates that determine freeze out will depend upon the  $\tilde{\gamma}$  and  $R^0$  masses, the cross sections involving the  $\tilde{\gamma}$  and  $R^0$ , and possibly the decay width of the  $R^0$  as well. In turn the cross sections and decay width also depend on the masses of the  $\tilde{\gamma}$ ,  $\tilde{g}$  and  $R^0$ , as well as the masses of the squarks and sleptons. We will denote the squark/slepton masses by a common mass scale (expected to be of order 100 GeV). Even if the masses were known and the short-distance physics specified, calculation of the width and some of the cross sections would be no easy task, because one is dealing with light hadrons. Fortunately, our conclusions are reasonably insensitive to individual masses, lifetimes, and cross sections, but depend crucially upon the  $R^0$ -to- $\tilde{\gamma}$  mass ratio, denoted by  $r$ . When we do need an explicit value of the photino mass  $m$ , the  $R^0$  mass  $M$ , or the squark/slepton mass  $M_{\tilde{S}}$ , we will parameterize them by the dimensionless parameters  $\mu_8$ ,  $r$ , and  $\mu_S$ :

$$m = 800\mu_8 \text{ MeV}; \quad M = rm; \quad M_{\tilde{S}} = 100\mu_S \text{ GeV}. \quad (2.3)$$

The standard procedure for the calculation of the present number density of a thermal relic of the early universe is to assume that the particle species was once in thermal equilibrium until at some point the rates for self-annihilation and pair-creation processes became much smaller than the expansion rate, and the particle species effectively froze out of equilibrium. After freeze out, its number density decreased only because of the dilution due to the expansion of the universe.

Since after freeze out the number of particles in a *comoving* volume is constant, it is convenient to express the number density of the particle species in terms of the entropy density, which in a comoving volume element is also constant for most of the history of the universe. This number-density-to-entropy ratio is usually denoted by  $Y$ . If a species of mass  $m$  is in equilibrium and nonrelativistic,  $Y$  is given simply in terms of the mass-to-temperature ratio  $x \equiv m/T$  as  $Y_{EQ}(x) = 0.145(g/g_*)x^{3/2} \exp(-x)$ , where  $g$  is the number of spin degrees of freedom, and  $g_*$  is the total number of relativistic degrees of freedom in the universe at temperature  $T = m/x$ . Well after freeze out  $Y(x)$  is constant—we will denote this asymptotic value of  $Y$  as  $Y_\infty$ .

If self annihilation determines the final abundance of a species,  $Y_\infty$  can be found by integrating the Boltzmann equation (dot denotes  $d/dt$ )  $\dot{n} + 3Hn = -\langle |v|\sigma_A \rangle (n^2 - n_{EQ}^2)$ , where  $n$  is the number density,  $n_{EQ}$  is the equilibrium number density,  $H$  is the expansion rate of the universe, and  $\langle |v|\sigma_A \rangle$  is the thermal average of the annihilation rate.

There are no general closed-form solutions to the Boltzmann equation, but there are reliable, well tested approximations for the late-time solution, i.e.,  $Y_\infty$ . Then with knowledge of  $Y_\infty$ , the contribution to  $\Omega h^2$  from the species can easily be found. Let us specialize to the survival of photinos assuming self-annihilation determines freeze out.

Calculation of the relic abundance involves first calculating the freeze-out value of  $x$ , known as  $x_f$ , where the abundance starts to depart from the equilibrium abundance. Using standard approximate solutions to the Boltzmann equation gives  $x_f = \ln(0.0481 m_{Pl} m \sigma_0) - 1.5 \ln[\ln(0.0481 m_{Pl} m \sigma_0)]$ , where we have used  $g = 2$ ,  $g_* = 10$ , and parameterized the nonrelativistic annihilation cross section as  $\langle |v|\sigma_A \rangle = \sigma_0 x^{-1}$ . Using the diagram shown in Figure 1,  $\sigma_0 = 2 \times 10^{-11} \mu_8^2 \mu_S^{-4} \text{ mb}$ , which leads to  $x_f \simeq 12.3 + \ln(\mu_8^3/\mu_S^4)$ . The value of  $x_f$  determines  $Y_\infty$ :

$$Y_\infty = \frac{2.4x_f^2}{m_{Pl} m \sigma_0} \simeq 7.4 \times 10^{-7} \mu_8^{-3} \mu_S^4. \quad (2.4)$$

Once  $Y_\infty$  is known, the present photino energy density can be easily calculated:  $\rho_{\tilde{\gamma}} = mn_{\tilde{\gamma}} = 0.8 \mu_8 \text{ GeV} \cdot Y_\infty 2970 \text{ cm}^{-3}$ . When this result is divided by the critical density,

$\rho_C = 1.054h^2 \times 10^{-5} \text{ GeV cm}^{-3}$ , the fraction of the critical density contributed by the photino is found to be  $\Omega_{\tilde{\gamma}}h^2 = 2.25 \times 10^8 \mu_8 Y_\infty$ . For  $Y_\infty$  in (2.4),  $\Omega_{\tilde{\gamma}}h^2 = 167\mu_8^{-2}\mu_S^4$ .

The age of the universe restricts  $\Omega_{\tilde{\gamma}}h^2$  to be less than one, so for  $\mu_S = 1$ , the photino must be more massive than about  $10^7 \text{ GeV}$  or so if its relic abundance is determined by self-annihilation.

### 2.3. $R^0$ -catalyzed freeze out

Farrar and I pointed out that for models in which both the photino and the gluino are light, freeze out is not determined by photino self annihilation, but by  $\tilde{\gamma} \longleftrightarrow R^0$  interconversion. The basic point is that since the  $R^0$  has strong interactions, it will stay in equilibrium longer than the photino, even though it is more massive. As long as  $\tilde{\gamma} \longleftrightarrow R^0$  interconversion occurs at a rate larger than  $H$ , then through its interactions with the  $R^0$ , the photino will be able to maintain its equilibrium abundance even after self annihilation has frozen out.

Griest and Seckel discussed the possibility that the relic abundance of the lightest species is determined by its interactions with another species. They concluded that the mass splitting between the relic and the heavier particle must be less than 10% for the effect to be appreciable. We find that  $\tilde{\gamma} \longleftrightarrow R^0$  interconversion determines the  $\tilde{\gamma}$  relic abundance even though the  $R^0$  may be twice as massive as the  $\tilde{\gamma}$ . The difference arises because Griest and Seckel assumed that all cross sections were roughly the same order of magnitude. But in our case the  $R^0$  annihilation is about  $10^{12}$  times larger than other relevant cross sections.

I will now consider in turn the reactions we found to be important in our scenario. The diagrams for the individual constituent processes can be found in Figure 1. However, as we shall see, it is not a simple task to go from the constituent diagrams to the cross sections and decay width.

$\tilde{\gamma}\tilde{\gamma} \rightarrow X$ : For photino self-annihilation at low energies the final state  $X$  is a lepton-antilepton pair, or a quark-antiquark pair which appears as light mesons. The process involves the  $t$ -channel exchange of a virtual squark or slepton between the photinos, producing the final-state fermion-antifermion pair. (See the upper third of Figure 1.) In the low-energy limit where the mass  $M_{\tilde{S}}$  of the squark/slepton is much greater than  $\sqrt{s}$ , the photino-photino-fermion-antifermion operator appears in the low-energy theory with a coefficient proportional to  $e_i^2/M_{\tilde{S}}^2$ , with  $e_i$  the charge of the final-state fermion. Also, as there are two identical fermions in the initial state, the annihilation proceeds as a  $p$ -wave, which introduces a factor of  $v^2$  in the low-energy cross section. The resultant low-energy photino self-annihilation cross section is:

$$\langle |v| \sigma_{\tilde{\gamma}\tilde{\gamma}} \rangle = 8\pi\alpha_{EM}^2 \sum_i q_i^4 \frac{m^2}{M_{\tilde{S}}^4} \frac{v^2}{3} \simeq 2.0 \times 10^{-11} x^{-1} [\mu_8^2 \mu_S^{-4}] \text{ mb}, \quad (2.5)$$

where we have used for the relative velocity  $v^2 = 6/x$  with  $x \equiv m/T$ , and  $q_i$  is the magnitude of the charge of a final-state fermion in units of the electron charge. For the light photinos we consider, summing over  $e$ ,  $\mu$ , and three colors of  $u$ ,  $d$ , and  $s$  quarks leads to  $\sum_i q_i^4 = 8/3$ .

$R^0 R^0 \rightarrow X$ : In  $R^0$  self-annihilation, at the constituent level the relevant reactions are  $\tilde{g} + \tilde{g} \rightarrow g + g$  and  $\tilde{q} + \tilde{q} \rightarrow q + \bar{q}$  (see the middle third of Figure 1), which are unsuppressed by any powers of  $M_{\tilde{S}}$ , so the cross section should be typical of strong interactions. In the nonrelativistic limit we expect the  $R^0 R^0$  cross section to be comparable to the  $\bar{p}p$  cross section, but with an extra factor of  $v^2$ , accounting for the fact that there are identical fermions in the initial state so annihilation proceeds through a  $p$ -wave. There is some en-

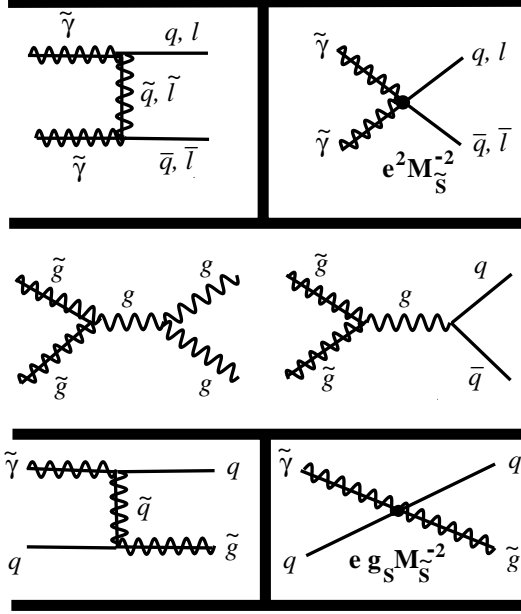


FIGURE 1. Feynmann diagrams for the constituent processes determining the relic photino abundance. The top left diagram is for  $\tilde{\gamma}$  self annihilation, and on the top right is the effective low-energy operator for that process. The two diagrams in the middle are the diagrams for  $R^0$  self annihilation. Finally in the lower left-hand corner is the  $\tilde{\gamma} \leftrightarrow R^0$  interconversion processes (all interconversion processes can be obtained from crossings of this diagram), and on the lower right-hand side is the effective low-energy operator.

ergy dependence to the  $\bar{p}p$  cross section, but it should be sufficient to consider  $\langle |v| \sigma_{R^0 R^0} \rangle$  to be a constant, approximately given by  $\langle |v| \sigma_{R^0 R^0} \rangle \simeq 100 v^2 \text{ mb} = 600 x^{-1} r^{-1} \text{ mb}$ , where we have used for the relative velocity  $v^2 = 6T/M = 6/(rx)$ , with  $x \equiv m/T$ .

We should note that the thermal average of the cross section might be even larger if there are resonances near threshold. In any case, this cross section should be much larger than any cross section involving the photino, and for the relatively small values of  $r$  we employ it will ensure that the  $R^0$  remains in equilibrium longer than the  $\tilde{\gamma}$ , greatly simplifying our considerations.

$\tilde{\gamma} R^0 \rightarrow X$ : This is an example of a phenomenon known as co-annihilation whereby the particle of interest (in our case the photino) disappears by annihilating with another particle (here, the  $R^0$ ). Of course co-annihilation also leads to a net decrease in  $R$ -odd particles. We can estimate the cross section for  $\tilde{\gamma} R^0 \rightarrow X$  in terms of the  $\tilde{\gamma}$  self annihilation cross section by comparing the lower third of Figure 1 to the upper third:

$$\langle |v| \sigma_{\tilde{\gamma} R^0} \rangle \simeq \frac{\alpha_S}{\alpha_{EM}} \frac{4}{3} \frac{2}{8/3} \frac{M}{m} \frac{3}{v^2} \langle |v| \sigma_{\tilde{\gamma}\tilde{\gamma}} \rangle, \quad (2.6)$$

where the ratio of  $\alpha$ 's arises because the short-distance operator for co-annihilation is proportional to  $e_i^2 g_S^2$  rather than  $e_i^4$ , the second factor is the color factor coming from the gluino coupling, and the third factor comes from the ratio of  $\sum_i q_i^2 / \sum_i q_i^4$  for the participating fermions. We have replaced  $m^2$  appearing in (2.5) by  $mM$ , although the actual dependence on  $m$  and  $M$  may be more complicated. Finally, the annihilation is  $s$ -wave so there is no  $v^2/3$  suppression as in photino self-annihilation.

Although the short-distance physics is perturbative, the initial gluino appears in a light hadron, and there are complications in the momentum fraction of the  $R^0$  carried

Table I: Cross sections and the decay width used in the calculation of the relic photino abundance. The dimensionless parameters  $\mu_8$  and  $\mu_S$  were defined in (2.3), and  $\mathcal{F}(r)$  was defined below (2.9). The coefficients  $A$ ,  $B$ , and  $C$  reflect uncertainties involving the calculation of hadronic matrix elements.

Process	Cross section or width
$R^0$ self annihilation:	$\langle  v  \sigma_{R^0 R^0} \rangle$ $600 x^{-1} r^{-1}$ mb
$\tilde{\gamma}$ self annihilation:	$\langle  v  \sigma_{\tilde{\gamma}\tilde{\gamma}} \rangle$ $2.0 \times 10^{-11} x^{-1} [\mu_8^2 \mu_S^{-4}]$ mb
co-annihilation:	$\langle  v  \sigma_{\tilde{\gamma} R^0} \rangle$ $1.5 \times 10^{-10} r [\mu_8^2 \mu_S^{-4} A]$ mb
$R^0$ decay:	$\langle  v  \sigma_{R^0 \rightarrow \tilde{\gamma} \pi \pi} \rangle$ $2.0 \times 10^{-14} \mathcal{F}(r) [\mu_8^5 \mu_S^{-4} B]$ GeV
$\tilde{\gamma} - R^0$ conversion:	$\langle  v  \sigma_{R^0 \pi} \rangle$ $1.5 \times 10^{-10} r [\mu_8^2 \mu_S^{-4} C]$ mb

by the gluino and other non-perturbative effects. For our purposes it will be sufficient to account for the uncertainty by including in the cross section an unknown coefficient  $A$ , leading to a final expression

$$\langle |v| \sigma_{\tilde{\gamma} R^0} \rangle \simeq 1.5 \times 10^{-10} r [\mu_8^2 \mu_S^{-4} A] \text{ mb.} \quad (2.7)$$

$R^0 \rightarrow \tilde{\gamma} \pi^+ \pi^-$ : In what we call interconversion processes, there is an  $R$ -odd particle in the initial as well as in the final state. Although the reactions do not of themselves change the number of  $R$ -odd particles, they keep the photinos in equilibrium with the  $R^0$ s, which in turn are kept in equilibrium through their self annihilations. An example is  $R^0$  decay. It can occur via, e.g., the gluino inside the initial  $R^0$  turning into an antiquark and a virtual squark, followed by squark decay into a photino and a quark. In the low-energy limit the quark–antiquark–gluino–photino vertex can be described by the same type of four-Fermi interaction as in co-annihilation (see Figure 1). One expects on dimensional grounds a decay width,  $\Gamma_0 \propto \alpha_{EM} \alpha_S M^5 / M_S^4$ . The lifetime of a free gluino to decay to a photino and massless quark-(anti)quark pair was computed by Haber and Kane. However this does not provide a very useful estimate when the gluino mass is less than the photino mass.

In an attempt to account for the effects of gluino-gluon interactions in the  $R^0$ , which is necessary for even a crude estimate of the  $R^0$  lifetime, Farrar developed a picture based on the approach of Altarelli et al.: The  $R^0$  is viewed as a state with a massless gluon carrying momentum fraction  $x$ , and a gluino carrying momentum fraction  $(1-x)$ ,<sup>†</sup> having therefore an effective mass  $M\sqrt{1-x}$ . The gluon structure function  $F(x)$  gives the probability in an interval  $x$  to  $x+dx$  of finding a gluon, and the corresponding effective mass for the gluino. One then obtains the  $R^0$  decay width (neglecting the mass of final state hadrons):

$$\Gamma_0(M, r) = \Gamma_0(M, 0) \int_0^{1-r^{-2}} dx (1-x)^{5/2} F(x) f(1/r\sqrt{1-x}), \quad (2.8)$$

where in this expression the factor  $\Gamma_0(M, 0)$  is the rate for a gluino of mass  $M$  to decay to a massless photino, and  $f(y) = [(1-y^2)(1+2y-7y^2+20y^3-7y^4+2y^5+y^6)+24y^3(1-y+y^2)\log y]$  contains the phase space suppression which is important when

<sup>†</sup> Of course there should be no confusion with the fact that in the discussion of the  $R^0$  lifetime we use  $x$  to denote the gluon momentum fraction whereas throughout the rest of the paper  $x$  denotes  $m/T$ .

the photino becomes massive in comparison to the gluino. Modeling  $K^\pm$  decay in a similar manner underestimates the lifetime by a factor of 2 to 4. This is in surprisingly good agreement; however caution should be exercised when extending the model to  $R^0$  decay, because kaon decay is much less sensitive to the phase-space suppression from the final state masses than the present case, since the range of interest will turn out to be  $r \sim 1.2 - 2.2$ . For  $r$  in this range, taking  $F(x) \sim 6x(1-x)$  leads to an approximate behavior

$$\sigma_{R^0 \rightarrow \tilde{\gamma}\pi^+\pi^-} = 2.0 \times 10^{-14} \mathcal{F}(r) \text{ GeV} [\mu_8^5 \mu_S^{-4} B], \quad (2.9)$$

where  $\mathcal{F}(r) = r^5(1-r^{-1})^6$ , and the factor  $B$  reflects the overall uncertainty. We believe a reasonable range for  $B$  is  $1/30 \lesssim B \lesssim 3$ . Lattice QCD calculation of the relevant hadronic matrix elements would allow a more reliable determination of  $B$ .

$R^0\pi \rightarrow \tilde{\gamma}\pi$ : The short-distance subprocess in this reaction is  $q + \tilde{g} \rightarrow q + \tilde{\gamma}$ , again described by the same low-energy effective operator as in co-annihilation and  $R^0$  decay. At the hadronic level the matrix element for  $R^0\pi \rightarrow \tilde{\gamma}X$  is the same as for  $R^0\tilde{\gamma} \rightarrow \pi X$  for any  $X$ , evaluated in different physical regions. Thus the difference between the various cross sections is just due to the difference in fluxes and final state phase space integrations, and variations of the matrix element with kinematic variables. Given the crude nature of the analysis here, and the great uncertainty in the overall magnitude of the cross sections, incorporating the constraints of crossing symmetry are not justified at present. We will therefore use the same form as for (2.7), letting  $C$  parameterize the hadronic uncertainty in this case:  $\langle |v| \sigma_{R^0\pi} \rangle \simeq 1.5 \times 10^{-10} r [\mu_8^2 \mu_S^{-4} C]$  mb.

This completes the discussion of the lifetimes, cross sections, and their uncertainties. The results are summarized in Table I.

Once the cross sections and decay rate is known, one can develop the Boltzmann equations for the system and numerically solve them to find the relic abundance. This is being studied by Chung, Farrar, and Kolb. But for the purpose of illustrating the main issues, it will suffice to compare equilibrium reaction rates to the expansion rate near freeze out.

To obtain an estimate of when the rates will drop below the expansion rate, we will assume all particles are in LTE (local thermodynamic equilibrium). In LTE a particle of mass  $m$  in the nonrelativistic limit has a number density

$$n = \frac{g}{(2\pi)^{3/2}} (mT)^{3/2} \exp(-m/T) = \frac{g}{(2\pi)^{3/2}} (T/m)^{3/2} m^3 \exp(-m/T). \quad (2.10)$$

Here  $g$  counts the number of spin degrees of freedom, and will be 2 for the  $R^0$  and the  $\tilde{\gamma}$ . Of course all rates are to be compared with the expansion rate. In the radiation-dominated universe with  $g_* \sim 10$  degrees of freedom

$$H = 1.66 g_*^{1/2} T^2 / m_{Pl} = 2.8 \times 10^{-19} x^{-2} [\mu_8^2] \text{ GeV}. \quad (2.11)$$

There are two striking features apparent when comparing the magnitudes of the equilibrium reaction rates in Table II. The first feature is that the numerical factor in  $R^0 R^0 \rightarrow X$  is enormous in comparison to the other numerical factors. This simply reflects the fact that  $R^0$  annihilation proceeds through a strong process, while the other processes are all suppressed by a factor of  $M_S^{-4}$ .

The other important feature is the exponential factors of the rates. They will largely determine when the photino will decouple, so it is worthwhile to examine them in detail.

The exponential factor in  $\tilde{\gamma}\tilde{\gamma} \rightarrow X$  is simply  $\exp(-m/T)$ , which arises from the equilibrium abundance of the  $\tilde{\gamma}$ . It is simple to understand: the probability of one  $\tilde{\gamma}$  to find another  $\tilde{\gamma}$  with which to annihilate is proportional to the photino density, which contains a factor of  $\exp(-m/T) = \exp(-x)$  in the nonrelativistic limit.

Table II: The ratio of the equilibrium reaction rates to the expansion rate for the indicated reactions. Shown in  $[\dots]$  is the scaling of the rates with unknown parameters characterizing the cross sections and decay width.

Process	$\Gamma, \Gamma_{EQ}/H$	Scaling
$\tilde{\gamma}\tilde{\gamma} \rightarrow X$	$1.2 \times 10^7 x^{-1/2} \exp(-x)$	$[\mu_8^3 \mu_S^{-4}]$
$R^0 R^0 \rightarrow X$	$3.5 \times 10^{20} x^{-1/2} r^{1/2} \exp(-rx)$	$[\mu_8]$
$\tilde{\gamma} R^0 \rightarrow X$	$8.9 \times 10^7 x^{1/2} r^{5/2} \exp(-rx)$	$[\mu_8^3 \mu_S^{-4} A]$
$\tilde{\gamma} \pi^+ \pi^- \rightarrow R^0$	$7.1 \times 10^4 x^2 r^{3/2} \mathcal{F}(r) \exp[-(r-1)x]$	$[\mu_8^3 \mu_S^{-4} B]$
$\tilde{\gamma} \pi \rightarrow R^0 \pi$	$9.6 \times 10^6 x^{1/2} r^{5/2} \exp[-(r-1)x] \exp(-0.175 \mu_8^{-1} x)$	$[\mu_8^{3/2} \mu_S^{-4} C]$

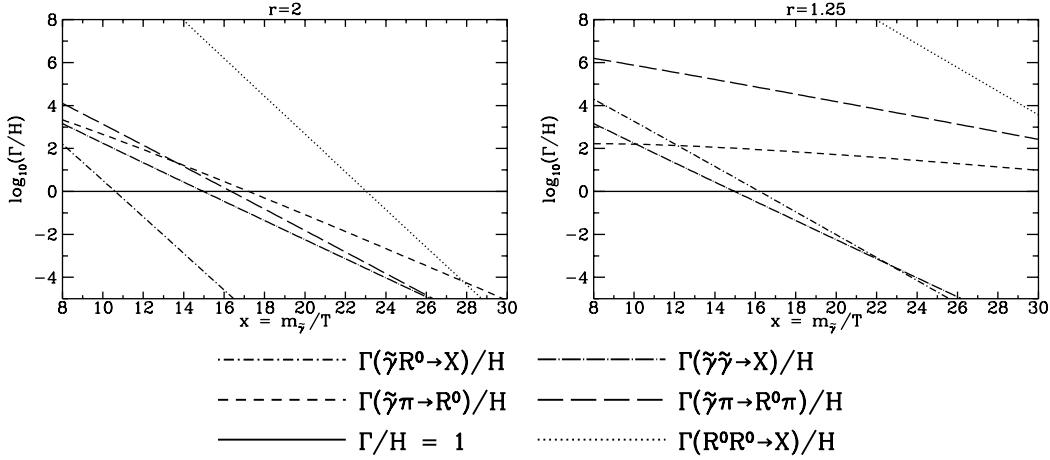


FIGURE 2. Equilibrium reaction rates divided by  $H$  for  $r = 1.25$  and  $r = 2.0$ , assuming  $\mu_8 = \mu_S = 1$ , and that the factors  $A = B = C = 1$ . The rates can be easily scaled for other choices of the parameters.

The similar exponential factor in  $R^0 R^0 \rightarrow X$  is also easy to understand. An  $R^0$  must find another  $R^0$  to annihilate, and that probability is proportional to  $\exp(-M/T) = \exp(-rx)$ .

The process  $\tilde{\gamma} R^0 \rightarrow X$  is also exothermic, so the only exponential suppression is the probability of a  $\tilde{\gamma}$  locating the  $R^0$  for co-annihilation, proportional to the equilibrium number density of  $R^0$ , which is proportional to  $\exp(-M/T) = \exp(-rx)$ .

In  $\tilde{\gamma} \pi^+ \pi^- \rightarrow R^0$  the exponential factor is  $\exp[-(M - m)/T] = \exp[-(r - 1)x]$ , which is just the “ $Q$ ” value of the decay process.

For the process  $\tilde{\gamma} \pi \rightarrow R^0 \pi$ , it is necessary for the collision to have sufficient center-of-mass energy to account for the  $\tilde{\gamma} - R^0$  mass difference, which accounts for a factor of  $\exp[-(M - m)/T]$ . The number density of target pions is  $\exp(-m_\pi/T)$ , so this factor is also present. Combining the two factors leads to the overall factor appearing in Table II:  $\exp[-(M - m + m_\pi)/T] = \exp[-(r - 1)x] \exp(-0.175 \mu_8^{-1} x)$ .

Graphs of the reaction rates as a function of  $r$  is shown in Figure 2. There are several things to notice from the graphs: 1) The  $R^0$  self-annihilation rate is always larger than the other rates. This means that the assumption that the  $R^0$  is in equilibrium during  $\tilde{\gamma}$

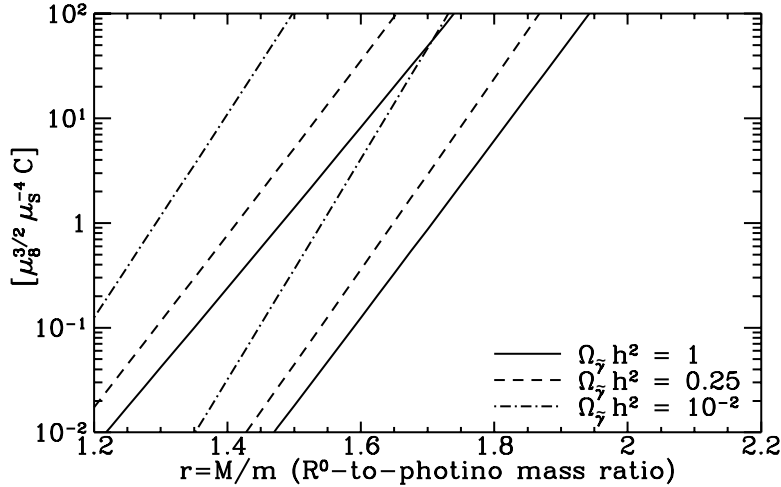


FIGURE 3. Assuming  $\tilde{\gamma}$  freeze out is determined by  $\tilde{\gamma} \leftrightarrow R^0$  interconversion, this figure shows as a function of  $r$  the values of  $[\mu_8^{3/2} \mu_S^{-4} C]$  required to give the indicated values of  $\Omega_{\tilde{\gamma}} h^2$ . The uncertainty band is generated by allowing  $\mu_8$  to vary independently over the range  $0.5 \leq \mu_8 \leq 2$ .

freeze out is a good approximation for the values of  $r$  considered here. 2) Even for  $r$  as large as  $r = 2$ , the interconversion rates seem to be (slightly) more important than  $\tilde{\gamma}$  self annihilation in keeping photinos in equilibrium. 3) The process  $\tilde{\gamma}\pi \leftrightarrow R^0\pi$  seems to be the most important process for  $r < 2$ . Detailed numerical integration of the Boltzmann equation by Chung, Farrar, and Kolb confirms this. 4) The freeze-out temperature is *very* sensitive to the value of  $r$ . This traces to the exponential sensitivity of the reaction rates upon  $r$ . We will make use of this last feature to find a cosmologically acceptable range of  $r$ .

Assuming that  $\tilde{\gamma}\pi \leftrightarrow R^0\pi$  does determine the  $\tilde{\gamma}$  relic abundance, Figure 3 shows the sensitivity of  $\Omega_{\tilde{\gamma}} h^2$  to  $r$ . From this figure we can draw some very interesting conclusions.

If we assume that  $[\mu_8^{3/2} \mu_S^{-4} C] < 10^2$ , then  $r$  must be less than 1.9. If we demand that the relic photinos are dynamically important (say  $\Omega_{\tilde{\gamma}} h^2 \geq 10^{-2}$ ) then  $r \geq 1.2$  if  $[\mu_8^{3/2} \mu_S^{-4} C] > 0.1$ . Finally, if we choose our best guess  $[\mu_8^{3/2} \mu_S^{-4} C] \sim 1$  and  $\Omega_{\tilde{\gamma}} h^2 \sim 0.25$ , then the allowed range of  $r$  is  $1.4 \lesssim r \lesssim 1.6$ .

#### 2.4. Testing the scenario

Direct detection of light photinos is not easy. the interaction cross section decreases with photinos mass, and more importantly, the kick they would give to a massive target nucleus also decreases with decreasing photino mass.

The case for light photinos hinges upon laboratory experiments. The scenario depends upon the existence of the  $R^0$ , the gluino—gluon bound state,† with a mass roughly 1.5 times the photino mass. If the  $R^0$  can be discovered (and after all, the discovery of a 1.5 GeV hadron does not sound impossible), from its decay one can learn the  $\tilde{\gamma}$  mass, and hence  $r$ , as well as the parameters of the short-distance matrix element. While there is no shortage of candidates for relic dark matter particle species, this proposal extends the idea that photinos may be the dark matter to a previously excluded mass range by incorporating new reactions that determine the photino relic abundance. If this scenario

† In fact, one suggested title for this talk is “The  $R^0$ : sglueball or screwball?”

is correct, direct and indirect detection of dark matter might be even more difficult than anticipated. However the scenario requires the existence of low-mass hadrons, which can be produced and detected at accelerators of moderate energy. Thus particle physics experiments will either disprove this scenario, or make light photinos the leading candidate for dark matter.

So the next step is obvious: find the  $R^0$ :

### 3. Relic axions

#### 3.1. *The axion*

The axion story begins with PQ symmetry breaking, which occurs when a complex scalar field  $\vec{\phi}$  with non-zero PQ charge develops a vacuum expectation value. This PQ symmetry breaking can be modeled by considering a potential of the standard form  $V(\vec{\phi}) = \lambda \left( |\vec{\phi}|^2 - f_a^2/2 \right)^2$ . The axion is the Nambu–Goldstone degree of freedom resulting from spontaneous breaking of the global symmetry. However, since the PQ symmetry is anomalous, it is broken explicitly by QCD instanton effects, leading to a mass for the axion. In general the instanton effects respect a residual  $Z_N$  symmetry, and the axion develops a potential due to instanton effects of the form  $V(a) = m_a^2 (f_a/N)^2 [1 - \cos(Na/f_a)]$ , where  $m_a = \Lambda_{QCD}/f_a$ . The axion field is often represented in terms of an angular variable  $\theta \equiv Na/f_a$ , and if  $\theta$  is taken as the dynamical variable, its potential (for  $N = 1$ ) is

$$V(\theta) = m_a^2(T) f_a^2 (1 - \cos \theta). \quad (3.12)$$

The above description is only valid at zero temperature. Because QCD instantons are large, with a size set by  $\Lambda_{QCD}^{-1}$ , their effects are strongly suppressed at high temperatures. Thus, after PQ symmetry breaking at  $T \sim f_a$ , but before QCD effects are important around  $T_{QCD}$ , the axion is effectively massless. For  $T \gg \Lambda_{QCD}$ , the temperature dependence of the axion mass scales as  $m_a^2(T) \propto (T/T_*)^{-n}$ , where  $n = 7.4 \pm 0.2$

#### 3.2. *The standard scenario*

When the field  $\theta(x)$  is created during the Peccei–Quinn symmetry breaking phase transition at  $T \sim f_a$ , it should be uncorrelated on scales larger than the Hubble radius at that time.

The usual assumption in axion cosmology is that PQ symmetry is broken before or during inflation, and the reheat temperature after inflation is too low to restore the PQ symmetry. This would mean that inflation will “smooth” the axion field on scales larger than the Hubble radius today. While this may indeed be the case, I will not make that assumption here. Since Tkachev and I first did the work reported here, Kofman, Linde, and Starobinski, as well as Tkachev, have made the interesting observation that symmetry restoration and breaking in the *preheating* phase of inflation may have interesting effects. Just one of the interesting effects may be to restore PQ symmetry after inflation, even if the reheat temperature is too low to do so. This means that PQ symmetry will be restored and broken after inflation, producing a spatially dependent axion field. While the dust has yet to settle on the issue, it is clear that it is naïve to think that inflation automatically results in a smooth axion field. So it is worthwhile to explore the possibility that the axion field is misaligned on scales larger than the Hubble radius at the time of the QCD transition when the axion mass switches on. In this part of the talk† I would

† Reference to all the material presented here can be found in Kolb and Tkachev (1993, 1994, 1996)

like to propose another different picture for the wanted poster: axions that are clumped today within our galaxy, rather than uniformly distributed.

Assuming an initially chaotic axion field after the PQ transition, as the temperature decreases and the Hubble radius grows the field becomes smooth on scales up to the Hubble radius. This continues until  $T = T_1 \sim 1$  GeV when the axion mass “switches on,” i.e., when  $m_a(T_1) \approx 3H(T_1)$ , and the axion mass begins to become important in the equations of motion. Coherent axion oscillations then transform fluctuations in the initial amplitude of the axion field into fluctuations in the axion density.

Since the initial amplitude of the coherent axion oscillations on the scale of the Hubble radius is uncorrelated, one expects that typical positive density fluctuations on this scale will satisfy  $\rho_a \approx 2\bar{\rho}_a$ , where  $\bar{\rho}_a$  is mean cosmological density of axions. These overdense regions were called axion miniclusters by Hogan and Rees. At the temperature of equal matter and radiation energy density,  $T_{\text{EQ}} = 5.5 \Omega_a h^2 \text{ eV}$ , non-linear fluctuations will separate out as miniclusters with  $\rho_{\text{MC}} \approx 10^{-14} \text{ g cm}^{-3}$ . The minicluster mass will be of the order of the axion mass within the Hubble radius at temperature  $T_1$ ,  $M_{\text{MC}} \sim 10^{-9} M_\odot$ . The radius of the cluster is  $R_{\text{MC}} \sim 10^{13} \text{ cm}$ , and the gravitational binding energy will result in an escape velocity of  $v_e/c \sim 10^{-8}$ .

It is easy to understand how a minicluster forms. First consider the evolution of the background axion density. In the limit that the initial misalignment angle is constant on all scales, the axion energy density scales with temperature as  $\bar{\rho}_a(T) = 3T_{\text{EQ}}s/4$  for  $T \ll \Lambda_{\text{QCD}}$ , where  $s \propto T^3$  is the entropy density and  $T_{\text{EQ}}$  is the temperature of equal matter and radiation energy densities.

Now suppose that there is a region with axion over-density,  $\rho_a = (1 + \Phi)\bar{\rho}_a$ . Then the matter density in that region will dominate the radiation density at a temperature  $T_\Phi = (1 + \Phi)T_{\text{EQ}}$ . If  $\Phi$  is larger than unity, then that region will separate out from the cosmological expansion, gravitationally collapse, relax, and form a minicluster with the approximate density it had at  $T_\Phi$ . A detailed study of this leads to a final minicluster density of

$$\rho_{mc} \simeq 140\Phi^3(1 + \Phi)\bar{\rho}_a(T_{e\text{q}}) \approx 3 \times 10^{-14}\Phi^3(1 + \Phi) (\Omega_a h^2)^4 \text{ g cm}^{-3}. \quad (3.13)$$

Even a relatively small increase in  $\Phi$  is important because the final density depends upon  $\Phi^4$  for  $\Phi \gtrsim 1$ .

### 3.3. *Non-linear axion dynamics and production of miniclusters*

Igor Tkachev integrated the field equations near the QCD transition with various choices for initial conditions where the axion field is inhomogeneous on scales larger than the Hubble radius.

In our numerical investigations of the dynamics of the axion field around the QCD epoch we found that as the oscillations commence, important, previously neglected, non-linear effects can result in the formation of transient soliton-like objects we called axitons. The non-linear effects result in regions with  $\Phi$  much larger than unity, possibly as large as several hundred, leading to enormous minicluster densities. We also found that the minicluster mass scale is set by the total mass in axions within the Hubble radius at a temperature around  $T = T_1 \approx 1$  GeV when axion mass is equal to  $H$ . Since this temperature is somewhat higher than  $\Lambda_{\text{QCD}}$ , the effect is to lower the minicluster mass from the estimate of Hogan and Rees to about  $10^{-12} M_\odot$ .

### 3.4. *Detecting axion miniclusters*

If a large fraction of axions end up in miniclusters (and in our numerical simulations that is what we found), then the local axion density may be very clumpy. This would mean

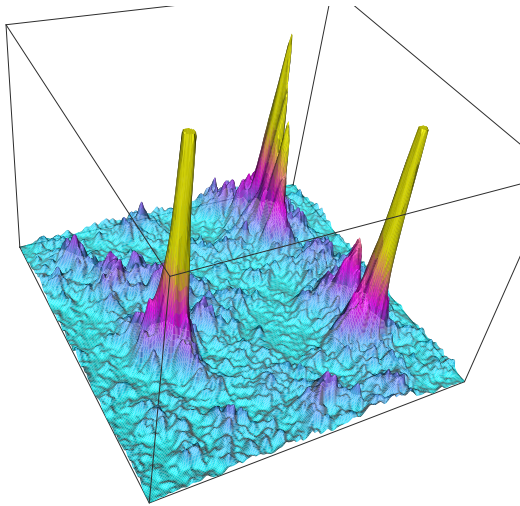


FIGURE 4. This is a two-dimensional slice through a three dimensional box of Tkachev's simulation showing the distribution of axion energy densities for  $T \gg T_{\text{eq}}$ . The height of the plot corresponds to  $\Phi = \delta\rho_a/\bar{\rho}_a = 20$ , and the width to a length of  $4H^{-1}(T_1)$  (this corresponds to a comoving length of about 0.25 pc). The miniclusters are clearly seen.

that direct searches for axions would not be very efficient unless we just happened to be passing through a minicluster.

However it may be possible to detect miniclusters through femtolensing or picolensing. The basic idea is that if gamma-ray bursts are at cosmological distances, then miniclusters could act as gravitational lenses. For source and lens of cosmological distances, the Einstein ring radius is  $R_E \sim 5 \times 10^{10} (M/10^{-12} M_\odot)^{1/2} \text{cm}$ . This means that if two gamma-ray burst detectors are separated by distances larger than  $R_E$ , typically one detector will be within the Einstein ring and the other will not. Measurement of different fluxes in two widely separated detectors would extend the detectable range of lens masses to  $M < 10^{-7} M_\odot$ . If the angular separation of the images of a point-like source is comparable to the wavelength of the light, interference between the lensed images will lead to a distinctive fringe pattern both in coordinate space and in energy spectrum. The interference pattern in the energy spectrum will depend upon the location of the detector. Since well separated detectors will see different patterns, there is a distinctive signature of the effect.

#### 4. Conclusions

Although there are solid, well motivated scenarios that lead to one of several suspects forming cold dark matter, one must explore vigorously the possibility of a non-standard scenario for standard dark-matter suspects (such as SUSY and axions). It would be a crime if we fail to apprehend dark matter just because a prime suspect appears in an unfamiliar guise.

I would like to acknowledge collaboration with Glennys Farrar and Daniel Chung on the light-photino work reported here, and collaborations with Igor Tkachev on the axion-minicluster work. This work was supported by the Department of Energy and by NASA under Grant NAG5-2788.

## REFERENCES

- FARRAR, G. R. & KOLB, E. W. 1996 Light photinos as dark matter. *Phys. Rev. D* **53**, 2990–3001.
- CHUNG, D. J. H., FARRAR, G. R. & KOLB, E. W. 1996 Light photinos as dark matter II. *In preparation.*
- KOLB, E. W. & TKACHEV, I. I. 1993 Axion miniclusters and bose stars. *Phys. Rev. Lett.* **71**, 3051–3054.
- KOLB, E. W. & TKACHEV, I. I. 1994 Non-linear axion dynamics and formation of cosmological pseudo-solitons. *Ap. Phys. Rev. D* **49**, 5040–5049.
- KOLB, E. W. & TKACHEV, I. I. 1996 Femtolensing and picolensing by axion miniclusters. *Ap. J. Lett.* **400**, L25–L29.